Composites: Part A 204 (2026) 109602

Contents lists available at ScienceDirect

Composites Part A

journal homepage: www.elsevier.com/locate/compositesa

Ultra-Thin interphase in Flax/Epoxy composites revealed by AFM PF-QNM nanomechanics

I. Arafat *, G. Colas, Y. Gaillard, L. Boubakar, V. Placet, F. Boutenel

Université Marie et Louis Pasteur, SUPMICROTECH, CNRS, Institut FEMTO-ST, F-25000 Besançon, France

HIGHLIGHTS

- The existence of a transition zone at the fibre/matrix interface is investigated.
- A near-field measurement technique is applied on a flax/epoxy composite.
- Nanomechanical AFM mappings finely assess the elastic properties of the interphase.
- An ultra-thin (around 80 nm) transition zone is observed and described.

GRAPHICAL ABSTRACT

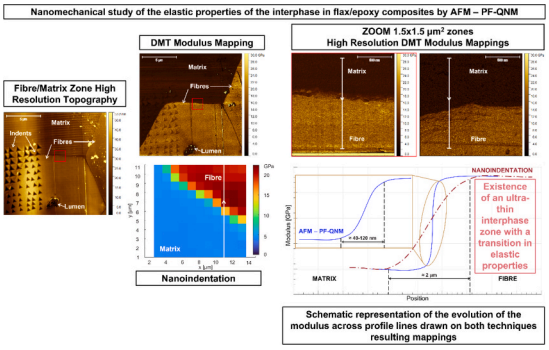

ARTICLE INFO

Keywords:
Flax fibres
DMT Modulus
Gradient of properties
Transition zone

ABSTRACT

The fibre/matrix interface is a critical yet poorly understood feature of natural-fibre-reinforced composites, where load transfer and damage initiation are controlled. At the nanoscale, this boundary may evolve into an interphase, a narrow region with a gradient of mechanical properties, but its occurrence in bio-based systems remains unclear. Here, we use Atomic Force Microscopy in PeakForce Quantitative Nanomechanical Mapping mode (AFM-PF-QNM) to directly probe the nanoscale elastic modulus across flax/epoxy interfaces. Systematic mappings of multiple fibres reveal that, under the present conditions, an interphase is not consistently formed. When present, it is extremely thin (≈ 40–120 nm) and exhibits a distinct modulus gradient. These findings provide the first nanoscale evidence of the ultra-thin and irregular nature of interphase formation in flax/epoxy composites, challenging the assumption of a uniform and thick interphase in plant-fibre systems and offering new insights for interface engineering.

1. Introduction

Environmental concerns are driving the development of sustainable composite materials, for which plant fibres such as flax represent promising alternatives to synthetic reinforcements due to their low density and favourable mechanical properties [1]. However, their complex ultrastructure and natural variability pose challenges for composite design [2].

* Corresponding author.
E-mail address: israa.arafat@femto-st.fr (I. Arafat).

https://doi.org/10.1016/j.compositesa.2026.109602
Received 10 November 2025; Received in revised form 9 January 2026; Accepted 23 January 2026
Available online 29 January 2026

The mechanical performance of fibre-reinforced composites is largely governed by the fibre/matrix interface, where load transfer occurs and where physico-chemical interactions during processing may lead to the formation of an interphase with graded properties [3–5]. While interfacial behaviour in flax-reinforced composites has been widely studied [5–7], the dimensional characteristics of the fibre–matrix interphase remain insufficiently explored. Le Duigou et al. [8] studied the case of flax fibres (Hermès and Electra) blended with a DGEBA/aliphatic amine system, using laser confocal microscopy. The polymerization occurred at 65°C for 14 h. They reported an interphase region 1.7 to 2.2 μm thick within the outer cell walls of the flax fibres. However, they did not investigate the interphase's properties, particularly its elastic behaviour.

Nanoindentation is a widely used technique to determine elastic properties at the micrometre scale. Gao and Mäder [9] employed phase imaging in Atomic Force Microscopy (AFM) tapping mode and nanoindentation to investigate the interphase formation of different composites. They discovered that unsized E-glass fibre/epoxy composites did not form an interphase. In contrast, sized E-glass fibre/epoxy composites exhibited an interphase approximately 300 nm wide, characterized by an elastic modulus gradient. Additionally, they examined sized-E-glass reinforced maleic-anhydride-grafted-polypropylene (PPm) and found an interphase with a different elastic modulus than the matrix, with a thickness ranging from less than 100 to about 300 nm. According to their findings, the interphase formation in all the studied composites was primarily attributed to the effects of the sizing. Li et al. [10] applied this technique on a sisal fibre/epoxy composite, and identified a transition zone between the fibres and the matrix without defining a thickness range. Similarly, Lee et al. [11] reported an interphase region approximately 1 μm thick in sized cellulose fibres/PPm composite. However, accurately quantifying the mechanical properties of such interphase regions using nanoindentation remains challenging. This difficulty arises from the influence of neighbouring materials' properties, the minimum required size and spacing of indents, and potential interpretation errors introduced during post-processing, particularly through interpolation [11,12].

AFM used in PeakForce Quantitative Nanomechanical Mapping™ mode (AFM – PF-QNM) is a recently developed technique that allows to precisely evaluate the mechanical properties of a material at nanometric resolution. This technique was used to study elastic properties in plant fibre cell walls. Arnould et al. [2] applied this technique to identify elastic modulus gradients between the cell walls of mature and developing flax fibres. Goudenhooft et al. [13] applied both nanoindentation and AFM – PF-QNM to compare the elastic properties of modern and ancient Egyptian flax fibres. Goudenhooft et al. [14] studied the evolution of the mechanical properties of flax fibres cell walls during the plant development. Similarly, Siniscalco et al. [15] applied AFM – PF-QNM to evaluate the temperature effects on the mechanical properties of the cell walls of elementary flax fibres, as well as those from flax/PP-MAPP and flax/PBS composites. Lastly, Arnould et al. [16] studied changes in the indentation modulus of poplar tension wood fibres cell wall layers during the maturation of the fibres.

Some studies applied AFM – PF-QNM to investigate the properties of the interphase region in glass/epoxy composites. Riaño et al. [3] studied the interphase formation in the case of a sized E-glass/DGEBA-based epoxy composite prepared by filament winding process. They discovered the existence of an interphase region about 200 nm thick, characterized by a decrease of around 35% of the matrix modulus.

However, to the best of authors' knowledge, no study applied AFM in PF-QNM mode to investigate the formation of an interphase zone with a transition in elastic modulus in the case of flax-fibre-reinforced composites.

The aim of this study is thus to investigate the elastic properties of the fibre/matrix interface of a flax/epoxy composite using AFM in PF-QNM mode to determine, at a fine scale, whether an interphase region with a gradient in elastic modulus exists. First, nanoindentation measurements were performed on one fibre/matrix zone for comparison with the AFM – PF-QNM measurements. Then, AFM – PF-QNM analyses were carried on multiple fibres of the same sample using three different scanning probes to study the interfacial properties of at the nanometre scale.

2. Materials and methods

2.1. Sample preparation

A 100x100 mm^2 sample with a thickness of 4 mm unidirectional (UD) composite sample was prepared for this study. UD flax fibres plies (FlaxTape™, Ecotechnilin, France) were used. The matrix was an epoxy system (Sicomin, France) obtained by the mixture of a partially biobased epoxy resin (SR GreenPoxy 56) and an amine hardener (SD 7561) in a 100:37 mass ratio. The composite was manufactured according to the protocol described by Cadu et al. [17], following a well-established and optimised procedure used by our team for over ten years. Applied to the system considered here (FlaxTape™, SR GreenPoxy 56, SD 7561), this process ensures a porosity content of below 3% and a fibre misalignment lower than 2-3°, while remaining representative of industrial manufacturing practices. Curing was performed by thermocompression for 1 h at 60°C and under a pressure of 3 bar. Post-curing occurred at 130°C for 1 h in an oven without pressure. The composite plate's volumetric composition was calculated by weighing method [17], and the volumetric void content was found to be of 2.4%.

Two 6x8x4 mm^3 samples were then laser cut. An ultramicrotome Leica Ultracut E (Leica Microsystems, Austria) was used with diamond knives (DiATOME, Switzerland) to prepare the surface to be studied by block face polishing: a DiATOME Histo knife was first used to remove semi-thin layers (500 nm), followed by a DiATOME ultra knife to remove ultra-thin layers (50 nm). Cutting was performed in dry conditions at a speed of 1 mm/s. It should be noted that tests were conducted on the ultramicrotomed surface of the bulk sample.

Fig. 1 presents schematic representations of a 100x100x4 mm^3 UD composite plate and two 6x8x4 mm^3 laser-cut samples, along with a numerical microscope image of the transverse cross-section of an ultramicrotomed sample. The image was captured with a VHX-5000 numerical microscope (Keyence, Japan). This transverse cross-section clearly reveals the typical microstructure of a unidirectional flax/epoxy composite, with individual elementary fibres and fibre bundles (containing from a few fibres to several tens of fibres) dispersed within the matrix. This level of fibre individualisation is characteristic of FlaxTape™ materials. The presence of cortical residues can also be observed in the vicinity of the largest fibre bundles, corresponding to residual impurities originating from the fibre separation process. The diameter of the elementary fibres ranges from a few micrometres to slightly more than twenty micrometres. A certain degree of heterogeneity in the spatial distribution of the fibres is also evident, with regions that are relatively resin-rich and others where the resin is more confined between fibres. In this study, the objective was to select fibres representative of these microstructural heterogeneities. A detailed explanation of the regions identified in Fig. 1-c is provided below.

In Fig. 1-c: A denotes a fibre within a bundle. B indicates a zone of confined resin, which means that the resin is confined between two or more fibres. C represents a single elementary flax fibre and D highlights a resin-rich area. Finally, O represents an optical shading which is relative to the surface preparation by Ultramicrotome.

For the Nanoindentation and AFM–PF-QNM measurements, ten fibres were selected to encompass all microstructural configurations. The chosen fibres were located in regions with minimal topographical artefacts, and specifically, those exhibiting small steps (≈ 4–15 nm) between the fibre and the surrounding matrix were selected to ensure accurate nanomechanical measurements.

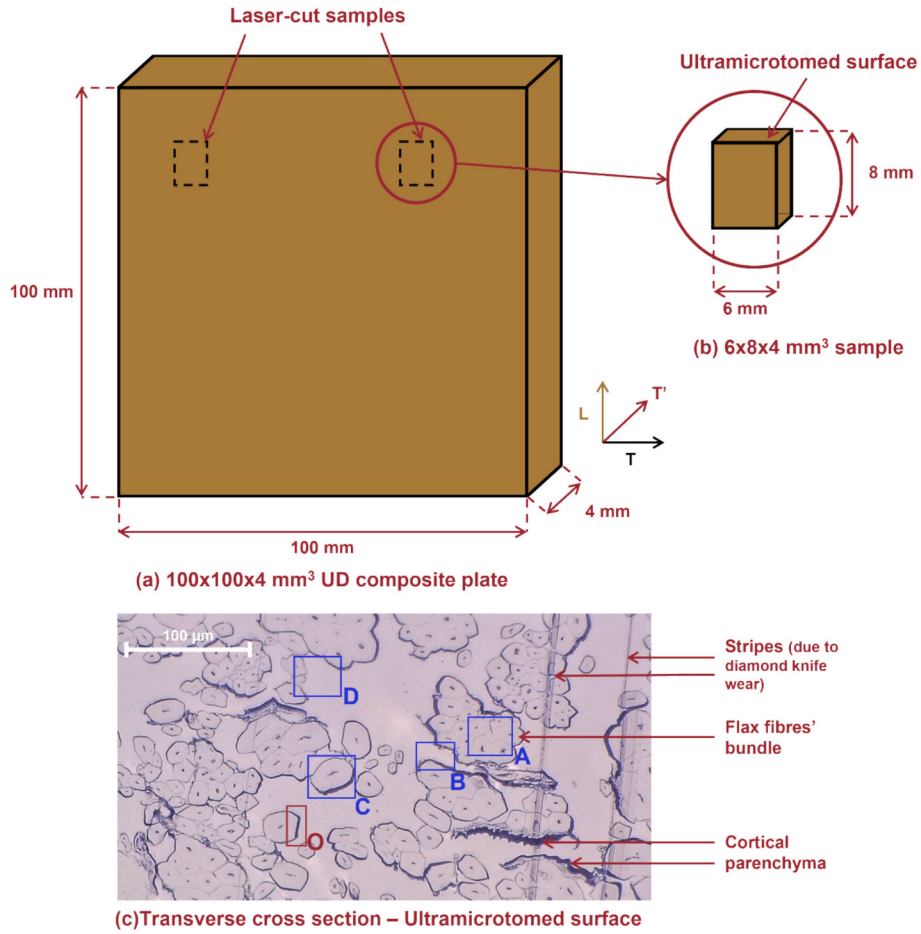

Fig. 1. Schematic representation of (a) a 100x100x4 mm^3 UD composite plate, and (b) a 6x8x4 mm^3 laser-cut sample. L represents the longitudinal direction (fibres' direction), T and T' represent the transverse directions. (c): Numerical microscope observation of an ultramicrotomed surface.

2.2. Nanoindentation

Nanoindentation measurements were carried at ambient conditions using an ultrananoindenter (UNHT) (Anton Paar, Austria), equipped with a Berkovich tip with a half angle of 65.3°. The shape area function has been calibrated using a material with a known Young's Modulus and Poisson's ratio (fused silica). A grid of 11x11 indentations was performed, maintaining a nominal distance of 1 µm between indents. The maximum load was set to 125 µN. The indentations were performed in dynamic mode following CSM + CAM method according to Liu et al. [18]. At maximum load, contact is maintained for 60 s, followed by the unloading phase, which is the same as described in [18]. This behaviour

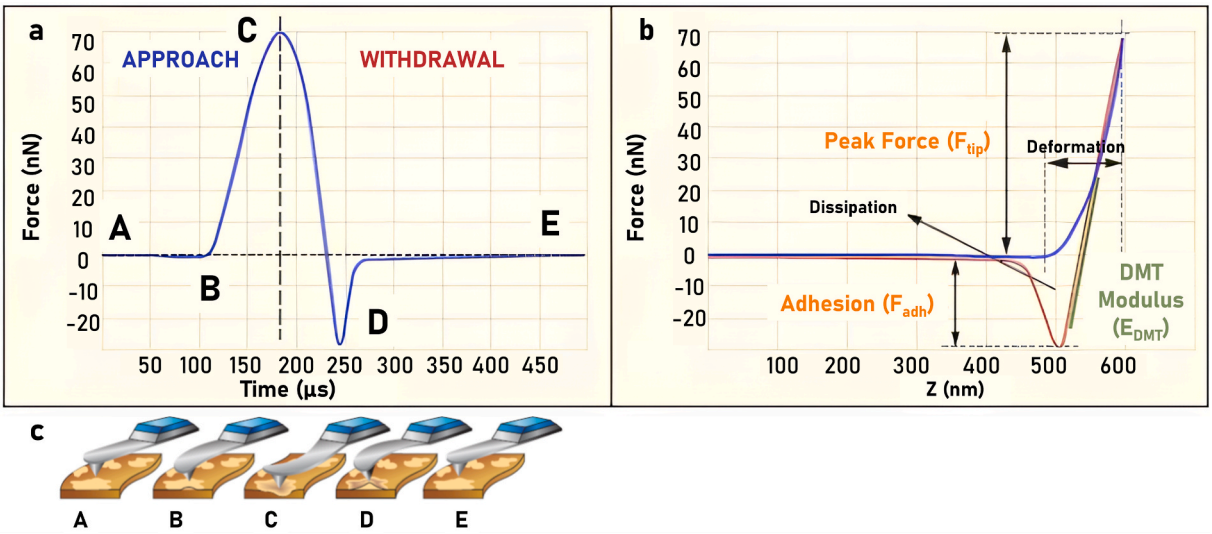

Fig. 2. Typical AFM – PF-QNM curves. a. Force-Time. b. Force-Displacement, Z is the tip-sample distance. c. Tip displacement [22].

suggests dynamic responses in the material, reflecting its viscoelastic properties, that will not be discussed in this study. Modulus values have been extracted on the unloading curve using the Oliver and Pharr Method [19], and mappings were drawn by nearest neighbour interpolation using MATLAB. Average modulus values were obtained using cumulative distribution function [20,21]. Poisson's ratio was set to 0.3.

2.3. AFM – PF-QNM

Quantitative nanomechanical AFM measurements were carried at ambient conditions (21°C and 45% Relative Humidity) on a Bruker Icon 5 device (Bruker, France). Fig. 2 shows a typical curve of an AFM – PF-QNM test along with the AFM tip's displacement. The tip approaches the surface while oscillating at a frequency far from its resonance frequency and comes into contact with the sample surface (phase A to B on Fig. 2-a). A frequency of 2 kHz was chosen for all the tests. The contact is maintained until maximum load (point C), followed by the withdrawal phase (C to D). Adhesion forces maintain the contact with the sample (point D) before the tip is fully withdrawn from the sample surface (point E). Usual AFM – PF-QNM measurements are done in the elastic regime, as the maximum depth of indentation is of a few nanometres, which means that the sample's surface remains intact after the test. Nanomechanical properties' mappings are acquired in real time.

Different scanning probes (Bruker, France) were used. First, a SCANASYST-AIR probe was used to carry out 15x15 μm^2 high-resolution (HR) topography mappings with 512x512 points. For the mechanical properties' mappings, a RTESPA-525-30 pre-calibrated probe with a tip radius of 32 nm and a cantilever stiffness of 305.91 nN/m was used. The measurement is performed at a maximum load of 200 nN, within the elastic range. Images of 15x15 μm^2 were acquired, with 512x512 points in each image. A measurement point is acquired every 29 nm. Then, a RTESPA-300 tip calibrated according to the Sader method [23] (https://sadermethod.org/) with a tip radius of 5 nm and a cantilever stiffness of 34.73 nN/m was used to map the nanomechanical properties of the interphase. Images of 1.5x1.5 μm^2 were acquired, with 512x512 points in each image. The tip radius was calibrated according to the matrix' modulus. A measurement point is acquired every 3 nm, with a maximum force of 30 nN. Cantilevers' sensitivity was calibrated using a reference sapphire sample provided by Bruker. Poisson's ratio was set to 0.3 for all the measurements.

Different contact models can be used to calculate the modulus [24]. By calculating the material's Tabor number (μ) (Eq. 1), and based on Johnson and Greenwood's adhesion map [25], we can define the most fitting contact model to be used for our measurements.

$$\mu = \left(\frac{R\Delta\gamma^2}{E^{*2}\epsilon^3}\right)^{1/3} \tag{1}$$

In Eq. 1:

μ is the Tabor number, R is the probe's radius, Δγ is the work of adhesion, E* is the combined modulus, and ϵ is the equilibrium spacing in the Lennard-Jones potential. Δγ and E* are given by Eq. 2 and Eq. 3, respectively.

$$\Delta\gamma = \frac{F_{adh}}{2\pi R} \tag{2}$$

$$E^* = \left(\frac{1-\nu_1^2}{E_1} + \frac{1-\nu_2^2}{E_2}\right)^{-1} \tag{3}$$

where F_{adh} is the adhesion force, R is the tip's radius, E_1 and ν_1 are the tip's Young Modulus and Poisson's ratio, and E_2 and ν_2 are the material's modulus and Poisson's ratio, respectively.

Tab. 1 presents the values used to calculate the flax fibres and the SR GreenPoxy matrix' respective Tabor numbers.

Accounting for $\epsilon = 0.3$ nm, we get $\mu_{Flaxfibres} = 0.0004$ and $\mu_{Matrix} = 0.0006$. Thus, the obtained Tabor numbers for both the flax fibres and the matrix are far inferior to 0.1, which means that, according to Johnson and Greenwood's adhesion map [25], Derjaguin-Muller-Toporov (DMT) contact model [26] can be used to calculate DMT Modulus (E_{DMT}) values from the withdrawal curve shown in Fig. 2 (Eq. 4).

Table 1
Materials' properties.

	Flax Fibres	SR GreenPoxy 56 + SD 7561 system	Single Crystal Si (RTESPA-300 probes)
Modulus (E_i) (GPa)	25	7	160
Poisson's ratio	0.3	0.3	0.3
Radius (nm)	–	–	5
Adhesion Force (nN)	25	16	–

$$F_{tip} = \frac{4}{3}E_{DMT}\sqrt{RD^3} + F_{adh} \tag{4}$$

Where F_{tip} refers to the selected Peak Force value, R is the tip radius and D is the tip-sample distance. F_{adh} is the adhesion force.

DMT's contact theory is commonly used in AFM – PF-QNM studies on natural fibres such as flax and wood [2,13–16]. It focuses on surface energy and adhesive forces, assuming spherical contact between rigid solids of small radius. However, the theory assumes isotropy and elastic behaviour, neglecting the directional dependence of material properties in anisotropic materials like flax fibres and the time-dependent behaviour of viscoelastic materials, which applies to both the fibres and the matrix. This oversight can result in inaccurate quantification of the materials' moduli. Nevertheless, as the main objective of this study is to quantitatively determine the fibre/matrix interface thickness, DMT's contact model will be utilised for modulus estimation, in accordance with Tabor number calculations and existing literature.

Thus, the obtained nanomechanical properties' mappings were processed without filtering using Gwyddion software [27]: mean DMT Modulus values and standard deviations were calculated by applying a Gaussian fit to the distributions of DMT Modulus values in masked regions of the images. Masks were drawn separately for the fibre and the matrix. It is important to note that measurement artefacts and interface regions were excluded from the masks. A total of 161 ± 15 points were included in the masks for the fibre regions, while 158 ± 21 points were included for the matrix regions.

For more clarity, Figs. S1 – S6 in the Supplementary data show the drawn masks, the exact number of points included in each mask, as well as the DMT modulus distribution along with the Gaussian fit for each masked region.

3. Results and discussions

Nanoindentation measurements were done to assess preliminary information on the modulus of the fibre and the matrix in a region of interest, and as a first approach to estimate the fibre/matrix interface thickness, aligning with insights from existing studies [9–11]. Fig. 3 shows the optical observation of the nanoindentation grid and the distribution of the modulus of the studied zone.

The mapping indicates a modulus value of 4.1 ± 0.2 GPa for the matrix and 20.1 ± 1.7 GPa for the fibre. These values are consistent with known resin properties and literature findings for the fibre [2,13]. These results will serve for comparison with AFM – PF-QNM measurements. Nevertheless, it should be noted that it is important to approach comparisons between the two techniques with caution, as there are significant differences, notably in the scanned volumes: in present nanoindentation measurements, the indentation depth ranges from approximately 60 to 120 nm, in the plastic domain, while in AFM – PF-

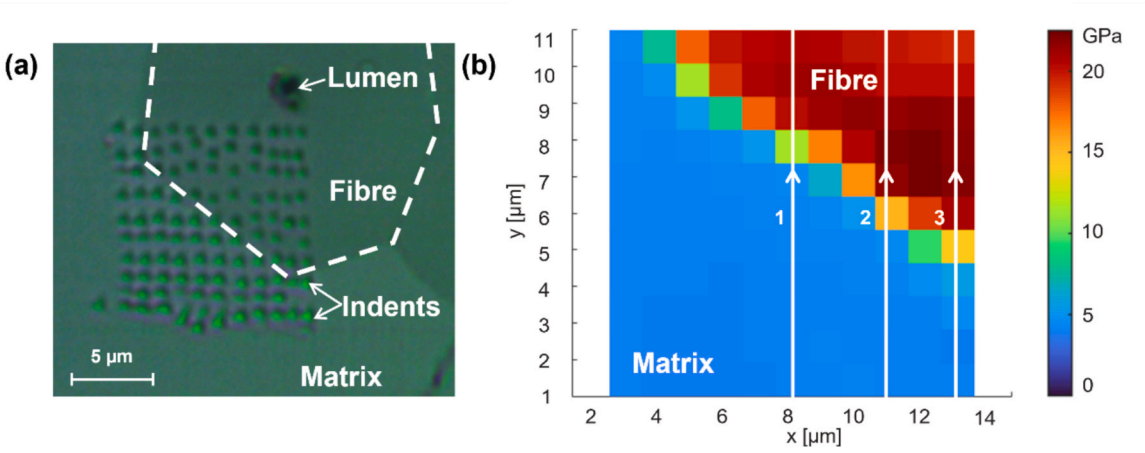

Fig. 3. (a) Optical image and (b) modulus mapping of a 11x11 indentation grid.

QNM measurements, the maximum indentation depth is of 5 nm, in the elastic domain. Moreover, nanoindentation involves multi-axial stress due to the indenter's geometry. Therefore, comparisons between AFM – PF-QNM and nanoindentation values should be made carefully.

Fig. 4 represents a graph showing the evolution of the modulus on three profile lines drawn on Fig. 3-b.

Thus, first AFM – PF-QNM measurements (Fig. 5) were performed on the zone shown in Fig. 3 (type A zone in section 2.1), in order to obtain HR topographical mappings of the zone, followed by nanomechanical measurements. The DMT Modulus mapping obtained (Fig. 5-b) reveals a DMT Modulus value of approximately 6.11 ± 1.1 GPa for the matrix and 17.09 ± 2.1 GPa for the fibre. These values are consistent with known resin properties and literature findings for the fibre [2,13], which allows us to validate the technique using a commonly employed spherical tip. However, no apparent micrometric transition zone was seen on the DMT Modulus mapping (Fig. 5-b). Therefore, following measurements will focus on studying the fibre/matrix interface using sharper tips (5 nm in radius) to achieve higher resolution in the measurement. To this end, new sets of measurements were performed on different 1.5x1.5 µm^2 fibre/matrix zones from the same sample, starting with the zone indicated by a red square in the mappings shown in Fig. 5. It should be noted that horizontal lines observed on the matrix region are due to slight jolting of the diamond knife during cutting, and the vertical lines mainly seen on the flax fibres' region are due to diamond knife wear.

All the 1.5x1.5 µm^2 images were acquired on zones from the same sample. The main obtained results are presented in Figs. 6-9 and will be discussed separately as different described zone types in section 2.1.

First, Fig. 6 illustrates the topography (a) and DMT Modulus (b) mappings for the area indicated by the red square in Fig. 5. This area is considered as a type A zone. Fig. 6-c displays a graph showing the evolution of both topography and DMT Modulus along the profile lines drawn on the mappings. The presented profiles each have a thickness of 10 pixels, representing the mean of ten consecutive 1-pixel lines. A total of 424 ± 32 points is included along each profile line. Table S1 in Supplementary data gives the exact number of points in each profile line for all the presented figures. It should be noted that the profile lines were drawn on the original, unedited real topography mapping. However, for visual clarity, the displayed topography mapping was realigned according to the fibre's plan after extracting the unedited topographical data for the profile lines. DMT Modulus values remain unchanged regardless of changes in topography mappings. Real unedited topography mappings are provided in Supplementary data (Figs. S7 – S12).

The same processing procedure was applied to all subsequent results. Fig. 6-b reveals that the DMT Modulus is of 17.71 ± 2.5 GPa for the fibre, and 7.02 ± 0.9 GPa for the matrix. Fig. 6-c highlights the existence of an ultra-thin transition zone about 115 nm wide between the fibre and the matrix. It can also be seen that the fibre's cell wall's properties are gradually increasing at the vicinity of the fibre/matrix interface.

The second case is a type B zone and is presented in Fig. 7. Fig. 7-a and b show the 15x15 µm^2 topography and DMT modulus mappings for

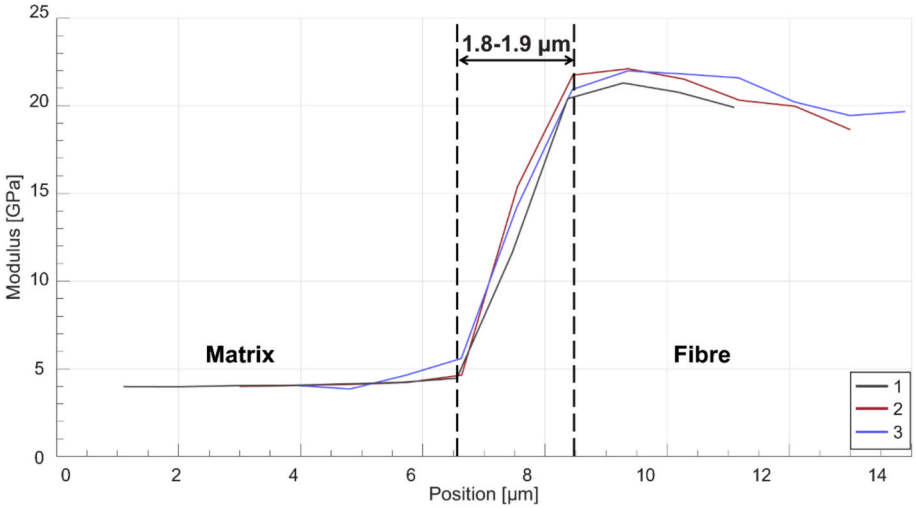

Fig. 4. Evolution of the modulus on the three profile lines drawn in Fig. 3-b.

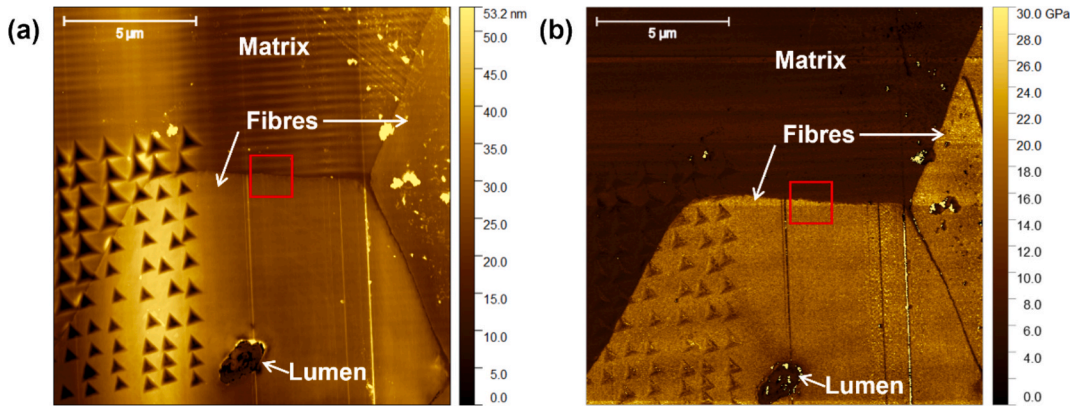

Fig. 5. (a) HR topography (obtained with SCANASYST-AIR) and (b) DMT Modulus mappings of a fibre/matrix zone of type A in a flax/epoxy composite (obtained with RTESPA-525–30).

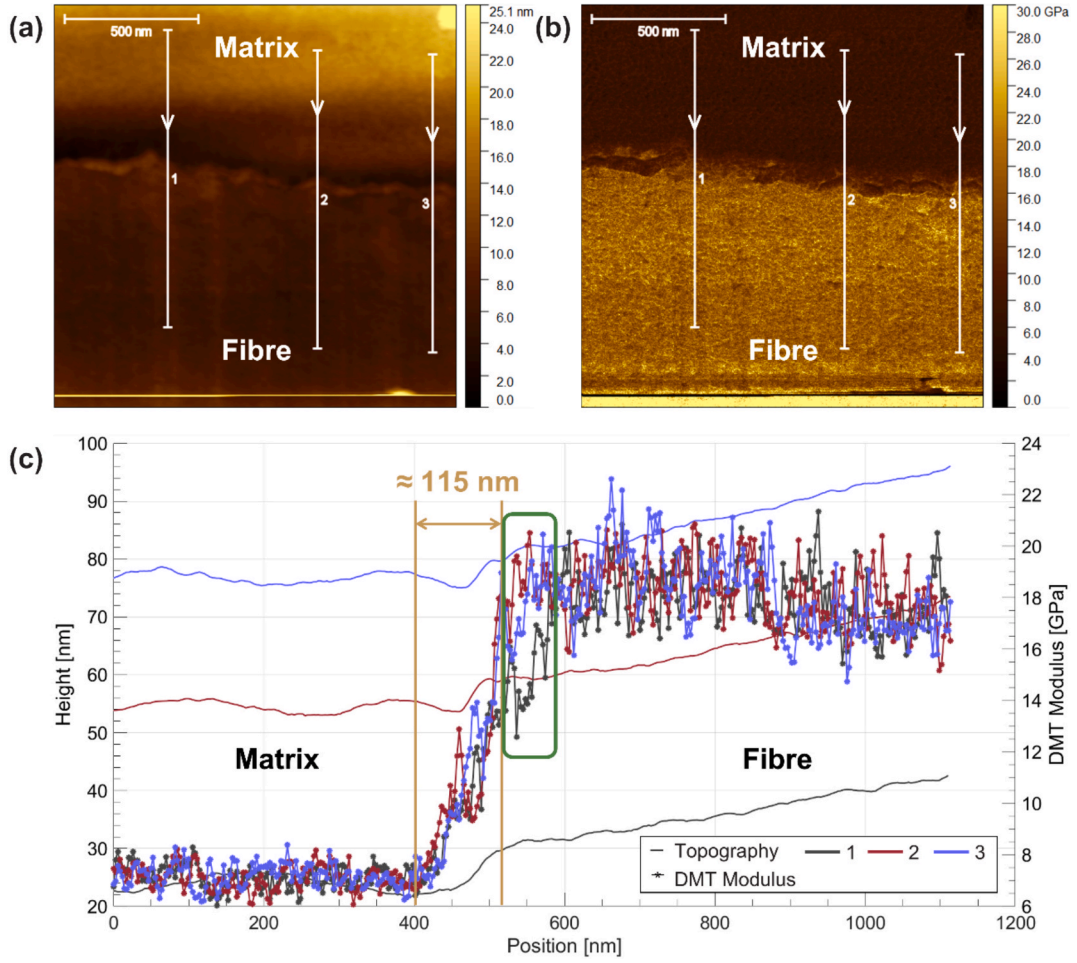

Fig. 6. PF-QNM mappings of (a) topography and (b) DMT Modulus of a 1.5x1.5 μm^2 fibre/matrix type A zone focusing on the fibre/matrix interface of a flax epoxy/ composite (obtained with RTESPA-300). (c) Evolution of the DMT Modulus and topography over the profile lines drawn on images (a) and (b).

this type B area. The DMT Modulus for the fibres appears to be of 13 ± 1.32, while it is of 5 ± 0.4 for the matrix. Again, no apparent micrometre transition zone is seen at the fibre/matrix interface. Fig. 7-c and d show the 1.5x1.5 μm^2 topography and DMT modulus mappings for the area indicated by a red square in Fig. 7-a and b. Horizontal lines observed on the fibres are due to diamond knife wear, and vertical lines on the matrix are due to slight jolting of the diamond knife during cutting. In this case, the DMT Modulus is of 4.94 ± 1.8 GPa for the matrix and 14.7 ± 2.7 GPa for the fibre. Fig. 7-e indicates that the presence of the interphase region is less prominent than in in the first case (Fig. 6-c), with a transition zone approximately only 36 nm wide.

Fig. 8-c displays an ultra-thin interphase region between the fibre and the matrix of about 43 nm in width for a type C zone. The obtained modulus values are of 8.71 ± 0.9 GPa for the matrix and 16.44 ± 2 GPa for the fibre. Moreover, a decrease in the matrix' properties in a zone about 100 nm wide at the vicinity of the fibre/matrix interface is

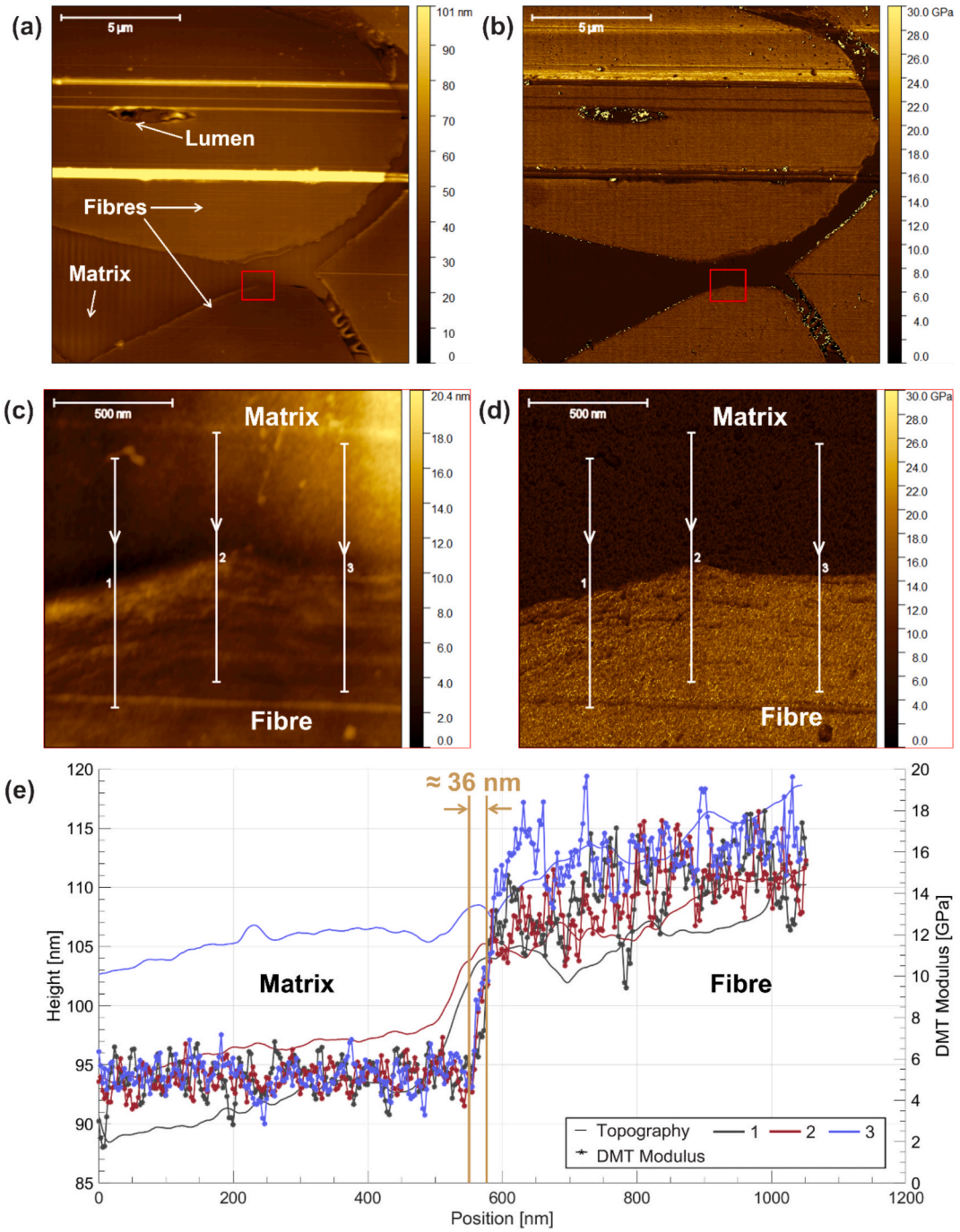

Fig. 7. PF-QNM mappings of (a) topography and (b) DMT Modulus of a 15x15 µm^2 fibre/matrix type B zone (obtained with RTESPA-525–30). (c) Topography and (d) DMT Modulus of the 1.5x1.5 µm^2 fibre/matrix type B zone indicated by red squares in images a and b, focusing on the fibre/matrix interface of a flax epoxy/composite (obtained with RTESPA-300). (e) Evolution of the DMT Modulus and topography over the profile lines drawn on images (c) and (d).

observed. It can also be seen that the properties of the flax fibre's cell wall slowly increase on a zone about 400 nm wide.

The last observed case is a type D zone and is presented in Fig. 9. The DMT Modulus is of 16.8 ± 2.9 GPa for the fibre and 7.14 ± 0.8 for the matrix. This time, a topographical effect can be seen at the fibre/matrix interface (Fig. 9-c), which hinders precise determination of the thickness of the apparently ultra-thin transition zone.

Thus, Fig. 10 summarises the AFM – PF-QNM results presented in this study. It is evident that, for the investigated system (FlaxTape^{TM} combined with SR GreenPoxy 56 and SD 7561 aliphatic amine hardener), and given the manufacturing process applied, a gradient in DMT Modulus is present within an ultra-thin transition zone between the fibre and the matrix.

As illustrated in Fig. 10, the data appear to represent a continuous range of interphase widths of approximately 40 to 120 nm. In other words, the presented cases lead us to the same conclusion that the transition zone's thickness falls within a narrow range, exceeding slightly only a hundred nanometres, with minor differences between the cases. Moreover, the ratio of the DMT modulus of the fibre to that of the matrix was 2.55 ± 0.37 across all measurements. This consistency indicates that the measurements are reliable and continuous. In the final case studied (shown in Fig. 9), a topographical effect does not allow for precise thickness quantification of the transition zone. In the first three cases, topographical effects do not seem to influence the observations, as

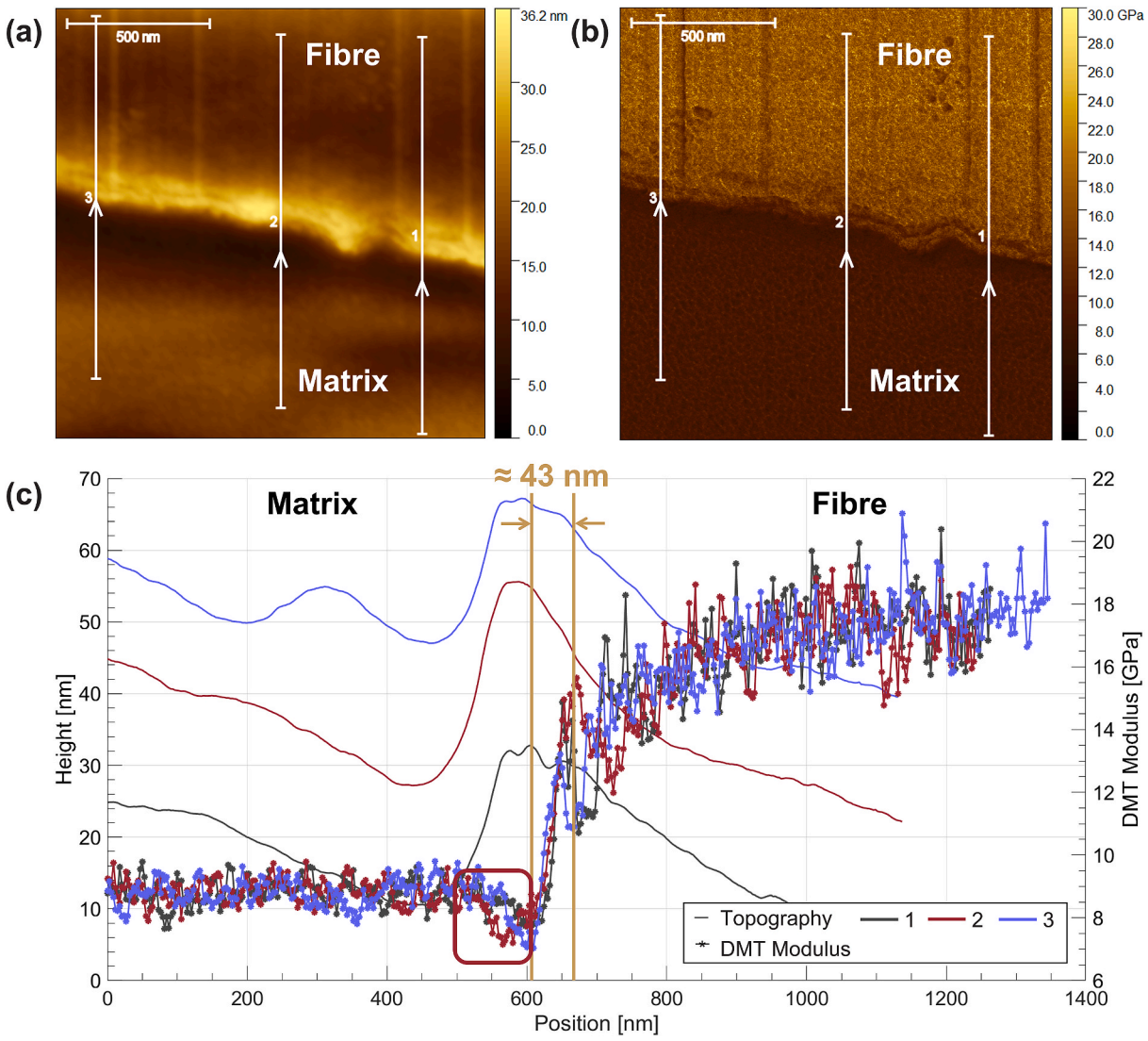

Fig. 8. PF-QNM mappings of (a) topography and (b) DMT Modulus of a 1.5x1.5 μm^2 fibre/matrix type C zone focusing on the fibre/matrix interface of a flax epoxy/composite (obtained with RTESPA-300). (c) Evolution of the DMT Modulus and topography over the profile lines drawn on images (a) and (b).

the DMT modulus evolution does not overlap with changes in local topography. Nonetheless, the collective results lead us to assert that, for this system, a micrometric transition zone does not appear to exist. These findings, obtained using a local near-field measuring technique at a spatial resolution of 3 nm per measurement point with a 10 nm diameter AFM probe, contrast with previous literature suggesting that the transition zone has a thickness of around 2 μm in flax/epoxy/aliphatic amine composites [8].

Consequently, Fig. 11 presents a summary diagram illustrating the obtained Nanoindentation and AFM – PF-QNM results.

All the above results underscore the importance of utilising local high-resolution near-field measuring techniques, such as AFM-PF-QNM, to accurately assess the interfacial characteristics of composite materials. Nanoindentation results align with existing literature works; nevertheless, it is important not to misinterpret the 1.8–1.9 μm wide region present between the fibre and the matrix (also shown in Fig. 4) as an interphase that is intrinsic to the composite's interfacial properties (yellow-orange pixels in Fig. 3-b). In fact, this area is where the indents engage with both materials (the fibre and the matrix), resulting in an apparent measured response that reflects the combined properties of the two. Although this interaction may suggest an averaging effect, it does not solely represent an interphase transition zone, as the measurements include contributions from both materials rather than purely interfacial characteristics. Additionally, the application of nearest neighbour interpolation further influences the results, leading to values that do not accurately depict the behaviour of the interphase itself. Therefore, this region should not be considered an interphase, but rather a cumulative effect of measurement and post-processing limitations. That is why it is necessary to analyse such transition zones using high-resolution quantitative local near-field techniques in order to obtain local information at the nanometre scale.

To the authors' knowledge, the obtained AFM – PF-QNM results are the first to demonstrate the existence of an ultra-thin transition zone measuring a few tens of nanometres in the case of flax/epoxy composites. Nonetheless, developing methods to quantitatively estimate the modulus values for both the fibres and the matrix is essential for further studies. These methods should rely on models that take into account the viscoelastic properties of the fibres and matrix, as well as the anisotropy of the flax fibres. By drawing inspiration from existing literature on this subject [28,29], more accurate approaches can be created, enhancing understanding and accuracy in modulus estimation. Furthermore, defining a zone as an interphase cannot solely rely on mechanical measurements of evolving elastic properties. A comprehensive understanding requires investigations into the chemical nature and the types

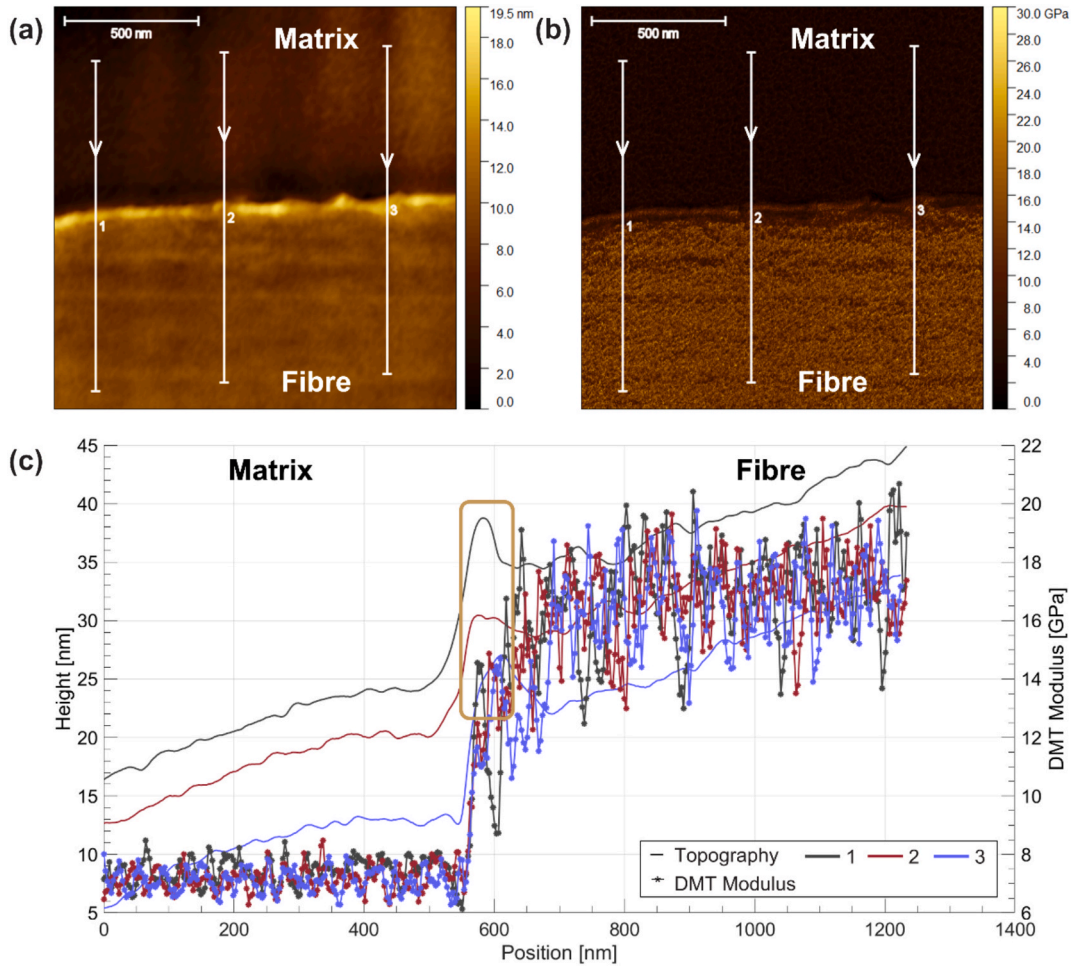

Fig. 9. PF-QNM mappings of (a) topography and (b) DMT Modulus of a 1.5x1.5 μm^2 fibre/matrix type D zone focusing on the fibre/matrix interface of a flax epoxy/ composite (obtained with RTESPA-300). (c) Evolution of the DMT Modulus and topography over the profile lines drawn on images (a) and (b).

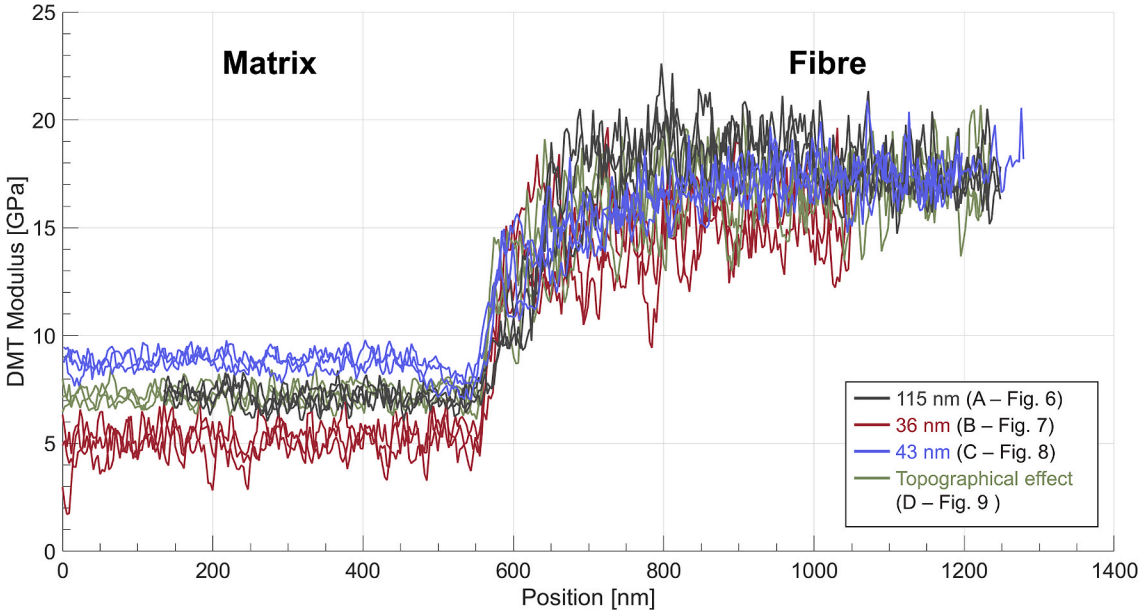

Fig. 10. Comparative graph of all DMT Modulus evolution curves for the presented results.

of locally present chemical bonds to accurately characterise what constitutes an interphase zone. With the present high-resolution nanomechanical measurements of DMT Modulus evolution, we have identified the existence of an ultra-thin transition region between the

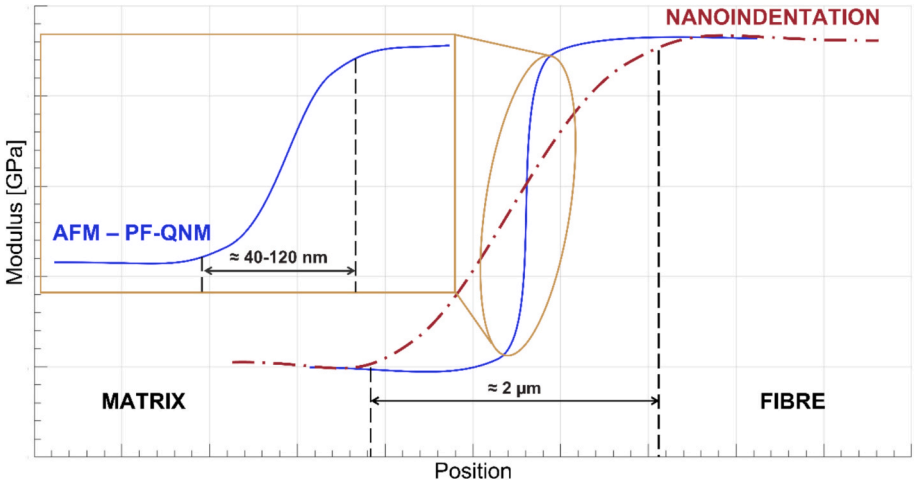

Fig. 11. Summary schematic representation of the obtained results.

fibre and the matrix. However, it remains uncertain whether this truly qualifies as an interphase with distinct local characteristics compared to the rest of the composite material. Therefore, studying the chemical nature of the environment and the locally existing chemical bonds is essential. The emergence of spectroscopic techniques with very high spatial resolution should allow these aspects to be documented in the near future. When coupled with nanomechanical results, a correlative spectro-mechanical spectroscopy approach can significantly enhance our understanding and improve our ability to define an interphase zone comprehensively, especially since the interfacial shear strength is generally high between flax fibres and the aliphatic amine/epoxy-based matrix, with reported values ranging from 13.2 to 22.5 MPa [8,30,31], which raises questions about the underlying adhesion mechanisms, as mechanical interlocking appears to be of secondary importance, as suggested by topographic cross-sections.

Moreover, further studies applying multi-scale approaches are essential for an overall understanding of the link between local nano-scale interfacial characteristics and macro-scale composite performance.

4. Conclusions

AFM in PF-QNM mode was used to study the existence of an interphase zone with a gradient of DMT Modulus in a flax/epoxy UD composite. Nanoindentation measurements were performed in alignment with existing literature studies. AFM PF-QNM measurements revealed that for the studied system (FlaxTape™, SR GreenPoxy 56 resin and SD 7561 aliphatic amine hardener) and in the conditions of the study (1.5x1.5 μm^2 mappings where a measurement point is acquired every 3 nm) the interactions that might occur between the fibres and the matrix result in the formation of an ultra-thin interphase region, with a thickness ranging from 40 to 120 nm, characterized by a transition from the DMT Modulus of the matrix to that of the fibre. Alternative fibre treatments such as sizing, modification of surface properties, or alterations in the nanoporosity of the fibre wall, as well as the use of different pre-polymers and hardeners with different physicochemical characteristics could result in distinct interphase properties. Further studies need to be performed on different fibre/matrix pairs, to obtain a better understanding of the behaviour of the interface. Moreover, studies correlating the behaviour of the composite material at the macroscopic scale to the interfacial behaviour at the nanometre scale are needed for a more global approach of the composite's behaviour. Alternatively, additional physico-chemical studies must complete the nanomechanical observations, in order to provide a wider comprehension of the different aspects of the multiphysical phenomena and interactions taking place at the fibre/matrix interface.

CRediT authorship contribution statement

I. Arafat: Writing – review & editing, Writing – original draft, Visualization, Validation, Methodology, Investigation, Formal analysis, Data curation, Conceptualization. **G. Colas:** Writing – review & editing, Validation, Methodology, Investigation, Funding acquisition, Formal analysis. **Y. Gaillard:** Writing – review & editing, Methodology, Data curation. **L. Boubakar:** Supervision, Conceptualization. **V. Placet:** Writing – review & editing, Validation, Supervision, Project administration, Conceptualization. **F. Boutenel:** Writing – review & editing, Validation, Supervision, Resources, Project administration, Funding acquisition, Conceptualization.

Declaration of competing interest

The authors declare that they have no known competing financial interests or personal relationships that could have appeared to influence the work reported in this paper.

Acknowledgements

This work, carried out as part of a thesis funded by a MESRI ministerial grant, received financial support from the Bourgogne-Franche-Comté Region, SUPMICROTECH and the CNRS. This research was also conducted as part of the EIPHI Graduate School (ANR-17-EURE-0002).

The authors of this article would also like to thank Joël Michel and Laure Avoscan (Plateforme DImaCell, Institut Agro Dijon, INRAE, Univ. Bourgogne Europe, F-21000 Dijon, France) for preparing the samples on the ultramicrotome, as well as the AMETISTE Platform facility (Institut FEMTO-ST, Besançon, France) for access to the Nanoindenter and the VHX-5000 numerical microscope, and the SURFACE Platform facility (Institut FEMTO-ST, Montbéliard, France) for access to the Bruker Icon 5 AFM device.

Appendix A. Supplementary data

Supplementary data to this article can be found online at https://doi.org/10.1016/j.compositesa.2026.109602.

Data availability

Data will be made available on request.

References

[1] Bourmaud A, Beaugrand J, Shah DU, Placet V, Baley C. Towards the design of high-performance plant fibre composites. Prog Mater Sci 2018;97:347–408. https://doi.org/10.1016/j.pmatsci.2018.05.005.

[2] Arnould O, Siniscalco D, Bourmaud A, Le Duigou A, Baley C. Better insight into the nano-mechanical properties of flax fibre cell walls. Ind Crop Prod 2017;97:224–8. https://doi.org/10.1016/j.indcrop.2016.12.020.

[3] Riaño L, Belec L, Chailan J-F, Joliff Y. Effect of interphase region on the elastic behavior of unidirectional glass-fiber/epoxy composites. Compos Struct 2018;198:109–16. https://doi.org/10.1016/j.compstruct.2018.05.039.

[4] Huang S, Fu Q, Yan L, Kasal B. Characterization of interfacial properties between fibre and polymer matrix in composite materials – a critical review. J Mater Res Technol 2021;13:1441–84. https://doi.org/10.1016/j.jmrt.2021.05.076.

[5] Canavy N, Rouilly A, Drouet C, Thouron C, Aufray M. Influence of flax fibers on epoxide-amine composites: Energetics of interphase formation. Polymer 2022;254:125047. https://doi.org/10.1016/j.polymer.2022.125047.

[6] Pantaloni D, Rudolph AL, Shah DU, Baley C, Bourmaud A. Interfacial and mechanical characterisation of biodegradable polymer-flax fibre composites. Compos Sci Technol 2021;201:108529. https://doi.org/10.1016/j.compscitech.2020.108529.

[7] Bellil S, Pantaloni D, Shah DU, Duigou AL, Baley C, Beaugrand J, et al. Prediction of interfacial behaviour of single flax fibre bonded to various matrices by simulation of microdroplet test. Compos C: Open Access 2023;11:100351. https://doi.org/10.1016/j.jcomc.2023.100351.

[8] Le Duigou A, Kervoelen A, Le Grand A, Nardin M, Baley C. Interfacial properties of flax fibre–epoxy resin systems: existence of a complex interphase. Compos Sci Technol 2014;100:152–7. https://doi.org/10.1016/j.compscitech.2014.06.009.

[9] Gao S-L, Mäder E. Characterisation of interphase nanoscale property variations in glass fibre reinforced polypropylene and epoxy resin composites. Compos A Appl Sci Manuf 2002;33:559–76. https://doi.org/10.1016/S1359-835X(01)00134-8.

[10] Li Q, Li Y, Zhou L. Nanoscale evaluation of multi-layer interfacial mechanical properties of sisal fiber reinforced composites by nanoindentation technique. Compos Sci Technol 2017;152:211–21. https://doi.org/10.1016/j.compscitech.2017.09.030.

[11] Lee S-H, Wang S, Pharr GM, Xu H. Evaluation of interphase properties in a cellulose fiber-reinforced polypropylene composite by nanoindentation and finite element analysis. Compos A Appl Sci Manuf 2007;38:1517–24. https://doi.org/10.1016/j.compositesa.2007.01.007.

[12] Gaillard Y, Amiot F. Grid nano-indentation as full-field measurements. Compos A Appl Sci Manuf 2020;132:105807. https://doi.org/10.1016/j.compositesa.2020.105807.

[13] Goudenhooft C, Durand S, Caër C, Melelli A, Magueresse A, Arnould O, et al. Complementarities of nanoindentation and atomic force microscopy for exploring micromechanical features of ancient flax fibres. Compos A Appl Sci Manuf 2025;190:108694. https://doi.org/10.1016/j.compositesa.2024.108694.

[14] Goudenhooft C, Siniscalco D, Arnould O, Bourmaud A, Sire O, Gorshkova T, et al. Investigation of the mechanical properties of flax cell walls during plant development: the relation between performance and cell wall structure. Fibers 2018;6:6. https://doi.org/10.3390/fib6010006.

[15] Siniscalco D, Arnould O, Bourmaud A, Le Duigou A, Baley C. Monitoring temperature effects on flax cell-wall mechanical properties within a composite material using AFM. Polym Test 2018;69:91–9. https://doi.org/10.1016/j.polymertesting.2018.05.009.

[16] Arnould O, Capron M, Ramonda M, Laurans F, Alméras T, Pilate G, et al. Mechanical characterisation of the developing cell wall layers of tension wood fibres by Atomic Force Microscopy. Peer Community J 2022;2:e39. https://doi.org/10.24072/pcjournal.138.

[17] Cadu T, Berges M, Sicot O, Person V, Piezel B, Van Schoors L, et al. What are the key parameters to produce a high-grade bio-based composite? Application to flax/epoxy UD laminates produced by thermocompression. Compos B Eng 2018;150:36–46. https://doi.org/10.1016/j.compositesb.2018.04.059.

[18] Liu T, Gaillard Y, Butaud P, Placet V, Ouisse M. In situ damping identification of plant fiber composites using dynamic grid nanoindentation. Compos A Appl Sci Manuf 2022;163:107158. https://doi.org/10.1016/j.compositesa.2022.107158.

[19] Oliver WC, Pharr GM. An improved technique for determining hardness and elastic modulus using load and displacement sensing indentation experiments. J Mater Res 1992;7:1564–83. https://doi.org/10.1557/JMR.1992.1564.

[20] Ulm F, Vandamme M, Bobko C, Alberto Ortega J, Tai K, Ortiz C. Statistical indentation techniques for hydrated nanocomposites: concrete, bone, and shale. J Am Ceram Soc 2007;90:2677–92. https://doi.org/10.1111/j.1551-2916.2007.02012.x.

[21] Tromas C, Arnoux M, Milhet X. Hardness cartography to increase the nanoindentation resolution in heterogeneous materials: Application to a Ni-based single-crystal superalloy. Scr Mater 2012;66:77–80. https://doi.org/10.1016/j.scriptamat.2011.09.042.

[22] Bruker Nano Surfaces and Metrology, Quantitative Imaging of Living Biological Samples Using PeakForce QNM. https://www.azonano.com/article.aspx?ArticleID=3026, 2023. (accessed 02 September 2025).

[23] Sader JE, Borgani R, Gibson CT, Haviland DB, Higgins MJ, Kilpatrick JI, et al. A virtual instrument to standardise the calibration of atomic force microscope cantilevers. Rev Sci Instrum 2016;87:093711. https://doi.org/10.1063/1.4962866.

[24] Shi X, Zhao Y-P. Comparison of various adhesion contact theories and the influence of dimensionless load parameter. J Adhes Sci Technol 2004;18:55–68. https://doi.org/10.1163/156856104322747009.

[25] Johnson KL, Greenwood JA. An Adhesion Map for the contact of Elastic Spheres. J Colloid Interface Sci 1997;192:326–33. https://doi.org/10.1006/jcis.1997.4984.

[26] Derjaguin BV, Muller VM, Toporov YUP. Effect of contact deformations on the adhesion of particles. J Colloid Interface Sci 1975;53:314–26. https://doi.org/10.1016/0021-9797(75)90018-1.

[27] Nečas D, Klapetek P. Gwyddion: an open-source software for SPM data analysis. Open Phys 2012;10:181–8. https://doi.org/10.2478/s11534-011-0096-2.

[28] Ganser C, Czibula C, Tscharnuter D, Schöberl T, Teichert C, Hirn U. Combining adhesive contact mechanics with a viscoelastic material model to probe local material properties by AFM. Soft Matter 2018;14:140–50. https://doi.org/10.1039/C7SM02057K.

[29] Czibula C, Ganser C, Seidlhofer T, Teichert C, Hirn U. Transverse viscoelastic properties of pulp fibers investigated with an atomic force microscopy method. J Mater Sci 2019;54:11448–61. https://doi.org/10.1007/s10853-019-03707-1.

[30] Le Duigou A, Davies P, Baley C. Interfacial bonding of Flax fibre/Poly(l-lactide) bio-composites. Compos Sci Technol 2010;70:231–9. https://doi.org/10.1016/j.compscitech.2009.10.009.

[31] Le Duigou A, Davies P, Baley C. Exploring durability of interfaces in flax fibre/epoxy micro-composites. Compos A Appl Sci Manuf 2013;48:121–8. https://doi.org/10.1016/j.compositesa.2013.01.010.